HHS Public Access

Author manuscript

J Child Neurol. Author manuscript; available in PMC 2022 December 01.

Published in final edited form as:

J Child Neurol. 2022 December ; 37(12-14): 927–938. doi:10.1177/08830738221114501.

Pilot study of associations among functional connectivity and neurocognition in survivors of pediatric brain tumor and healthy peers

Safiyah Seck[1], **Young Jin (Ginnie) Kim, B.S.**[1], **William A. Cunningham, Ph.D.**[2], **Randal Olshefski, M.D.**[3,4], **Keith Owen Yeates, Ph.D.**[5,6], **Kathryn Vannatta, Ph.D.**[1,4], **Kristen R. Hoskinson, Ph.D.**[1,4]

[1]Center for Biobehavioral Health, The Abigail Wexner Research Institute at Nationwide Children's Hospital, Columbus, OH

[2]University of Toronto, Ontario Canada

[3]Section of Hematology/Oncology/BMT, Nationwide Children's Hospital, Columbus, OH

[4]Department of Pediatrics, The Ohio State University College of Medicine, Columbus, OH

[5]Department of Psychology, University of Calgary, Calgary AB

[6]Alberta Children's Hospital Research Institute and Hotchkiss Brain Institute, University of Calgary, Calgary AB

Abstract

This pilot study examined the associations among functional connectivity in the salience (SN), central executive (CEN), and default mode networks (DMN), and neurocognition in pediatric brain tumor survivors (PBTS) and healthy children (HC). Thirteen PBTS (9 boys, M=12.76yr) and 10 HC (6 boys, M=12.70yr) completed MRI and assessment of processing speed and executive function. PBTS performed more poorly than HC on measures of processing speed, divided attention, and working memory; parent ratings of day to day executive function did not differ significantly by group, though both PBTS who underwent only surgical resection and HC were rated by parents as having difficulties approaching a standard deviation above the normative mean. Connectivity was lower in the SN and greater in the DMN in PBTS. Cross-method correlations showed that increased SN and DMN connectivity were associated with better task performance and parent-rated executive skills, and higher CEN connectivity with poorer parent-rated executive skills. This perhaps reflects an adaptive pattern of hyperconnectivity in PBTS.

Corresponding Author Information: Kristen R. Hoskinson, PhD, Center for Biobehavioral Health, The Abigail Wexner Research Institute at Nationwide Children's Hospital, 700 Children's Drive, Columbus, Ohio 43205, USA, Kristen.hoskinson@nationwidechildrens.org.

DECLARATION OF CONFLICTING INTERESTS

The authors declare that there are no conflicts of interest.

Note: a list of abbreviations contained in this manuscript is available in Supplementary Table 1.

Keywords

magnetic resonance imaging; brain tumor; cortical network; cognition; functional connectivity

INTRODUCTION

Childhood brain tumors are the most common solid tumor diagnosis and the second leading cause of cancer-related death in pediatric patients in the United States, affecting over 4,000 children under the age of 19 annually.[1] Fortunately, the 5-year survival rate among children and adolescents has reached 74.1%.[2] Nevertheless, chronic illnesses in early childhood are widely acknowledged to often have significant long-term sequelae that can carry into adulthood, including negative impacts on neurocognitive skills.[3] This is particularly true among those treated for chronic illnesses directly affecting brain systems. Survivors of pediatric brain tumor (PBTS) are unfortunately vulnerable to these negative outcomes, although debate continues regarding the mechanisms that underlie these so-called neurocognitive “late effects”, which occur across many domains, including intellectual functioning, executive function, memory, and academic achievement.[4]

Given the direct and indirect impacts of pediatric brain tumors on brain systems that contribute to cognition, behavior, and emotional functioning, direct examination of these systems is essential to identify the mechanisms underlying long-term morbidities. The salience network (SN) in particular may be highly relevant. This prominent neural network is rooted in the anterior insula and dorsal anterior cingulate cortex (see Figure 1a). Multiple studies across different populations show that the SN contributes to a variety of higher order brain functions that require the integration of complex information, including functions that involve the integration of multiple sensory, cognitive, and/or emotional inputs.[5–7] As a highly interconnected network, the SN interacts with other brain networks to facilitate complex skills like communication, social behavior, neurocognition, and self-awareness;[8] these skills are often compromised following pediatric brain tumor,[4] perhaps due to the impact of the tumor or its treatment on SN connectivity.[8]

The SN may be particularly important in modulating shifts between two other prominent networks, the fronto-parietal network (also termed the central executive network (CEN)) and the default mode network (DMN). In essence, once the SN has recognized the salience of a stimulus, it is responsible for signaling the activation of the CEN while suppressing activity within the DMN,[9] a synergistic system described as the “triple unifying networks”.[7] The CEN is anchored in the dorsolateral prefrontal cortex and posterior parietal cortex, and also involves the caudate nucleus and thalamus (see Figure 1b); CEN nodes show strong coactivation during cognitively challenging tasks, especially those that involve working memory, making judgments, and making decisions about actions or responses.[10] The DMN includes the medial temporal lobes and the angular gyrus, as well as the posterior cingulate and the ventromedial prefrontal cortex (see Figure 1c). These regions have been linked to complex neurocognitive processes like memory and social cognition, as well as to semantic processing.[10]

Magnetic resonance imaging (MRI) provides a critical means of examining the brain systems that likely contribute to the long-term consequences of pediatric brain tumor. *Functional* imaging methods are particularly critical to linking neural substrates and neurocognitive and behavioral outcomes. Resting-state fMRI (rsfMRI) allows for mapping of functional connectivity among different brain regions and provides the ability to examine large-scale brain networks, or regions of the brain that essentially coactivate.[11] It can provide insights into the associations among these networks, and subsequently draw links with abnormalities in behavior or cognition.

Importantly, despite calls for investigation of underlying mechanisms that contribute to the long-term consequences of pediatric brain tumor, MRI (particularly fMRI) is rarely integrated into studies of late effects in PBTS. Anandarajah and colleagues recently documented reduced within-network connectivity in the DMN and SN, and linked this reduced connectivity to reduced performance on the NIH Toolbox Cognitive measures.[12] In contrast, Chen and colleagues examined connectivity within the SN, CEN, and DMN in adult survivors of childhood brain tumor and noted increased strength and number of connections, and posited that this might reflect an increased need for higher effort by survivors, leading to greater recruitment of neighboring brain regions in frontal functional networks, which they termed an “all hands on deck” approach.[13] These contradictory findings highlight the need for further examination of these patterns in PBTS.

This pilot study, therefore, sought to examine the relationships among resting state functional activation in regions of the SN, CEN, and DMN, and neurocognition in PBTS and a cohort of their healthy peers. We hypothesized that survivors would have lower within-network connectivity compared to healthy peers. Additionally, we hypothesized that these brain-based differences would be associated with neurocognitive deficits as reflected by overall lower performance on cognitive assessments. Given the SN’s role in modulating the CEN and DMN in non-clinical populations, we also explored whether this expected pattern found in “triple unifying network” research[7] was also seen in PBTS. In all analyses, we examined group differences stratified by treatment modality.

PATIENTS AND METHODS

Participants and Procedures

Participants included 13 PBTS (9 boys) and 10 healthy children (HC; 6 boys). They were a subset of participants in a larger parent study examining social outcomes and neurocognition following treatment for pediatric brain tumor. Participants completing parent study visits in the final two years of the study period were screened for eligibility for the MRI protocol. Data collected during participation for the parent study included school- and home-based assessment of neurocognitive, adaptive, emotional, behavioral, and social functioning. Eligibility criteria for both groups included being from 9–14 years old, living within 120 miles of the hospital, and being fluent in English with at least 1 caregiver also fluent in English. Survivors were 2 or more years post-treatment for a primary, intracranial tumor without evidence of active, progressive disease. Survivors were excluded if they had a diagnosis of neurodevelopmental disorder prior to the brain tumor diagnosis, or had full-time special education placement. HC similarly could not have a history

of neurodevelopmental disorder or any chronic illness receiving treatment by a medical subspecialist for six months or longer. To be recruited for MRI, additional exclusion criteria included receiving inpatient treatment for a behavioral or psychiatric disorder, deficits in motor skills, vision, or hearing precluding completion of study measures, or having devices or orthodontics that either prevented or could distort image acquisition. Children were excluded due to braces/permanent retainer (PBTS=6; HC=4), implanted devices (PBTS=7), disinterest (PBTS=3; HC=7), requiring sedation for MRI (PBTS=1), or passive decline (PBTS=2; HC=8). Overall recruitment rates were 40.6% for PBTS and 34.5% for HC. Children excluded from the MRI component did not differ from those included based on age, sex, race or ethnicity. All participants were right-handed. Diagnostic and treatment information for PBTS are provided in Supplementary Table 2.

During their participation in the MRI study, parents and children provided written informed consent and assent, respectively, before study procedures commenced. All procedures were approved by the Institutional Review Board. Prior to MRI sessions, children were introduced to the MRI environment using a mock scanner to ensure comfort and ability to limit motion during image acquisition. The MRI session, which lasted approximately 50 minutes including preparation time, involved acquisition of volumetric, resting-state and task-based functional, and diffusion tensor sequences. Parents and children were compensated for their participation. Demographic, diagnostic and treatment information are summarized in Table 1. PBTS and HC did not differ from each other in age at participation, race, ethnicity, sex, parent marital status, parent education, or family income (all $ps > .05$). To account for the potential impact of tumor treatment on outcome measures, subsequent between group analyses and correlations of outcome measures treated group as multi-categorical (HC=10; PBTS, surgery-only=7; PBTS, surgery+adjuvant=6).

Measures

The Coding and Symbol Search subtests of the Wechsler Intelligence Scale for Children-Fourth Edition[14] were administered to measure processing speed. These well-validated and norm-referenced scales have strong psychometric properties, including high internal consistency ($\alpha = .88$), and contribute to the Processing Speed Index, which was used in analyses. This index is reported as a standard score, with a mean of 100 and standard deviation of 15, with higher scores indicating better performance.

Additionally, selected subtests from the Test of Everyday Attention for Children[15] were administered to assess aspects of attention and executive function. In this study, three subtests were administered: Walk Don't Walk (WDW), Code Transmission (CT), and Creature Counting (CC). WDW and CT measure sustained attention and CC measures switching attention. Test-retest reliability for measures of sustained attention ranges from $r = .71–.78$. CC also demonstrates high reliability ($r = .78$). These subtest scores are reported as scaled scores, with a mean of 10 and standard deviation of 3, with higher scores indicating better performance.

The Behavior Rating Inventory of Executive Function,[16] a parent-rated measure of children's executive function in the daily environment, was also administered. The BRIEF consists of eight clinical scales that are divided into two indexes: Behavioral Regulation

(three scales) and Metacognition (five scales). Behavioral Regulation includes Inhibit, Shift, and Emotional Control; Metacognition includes Initiate, Working Memory, Plan/Organize, Organization of Materials, and Monitor. Overall, the BRIEF shows both strong test-reliability (r = .82) and internal consistency (α = .80–.98). The Behavioral Regulation and Metacognition Index, and the General Executive Composite, are used in analyses and are reported as T scores, with a mean of 50 and standard deviation of 10, with higher scores indicating worse everyday executive functioning.

Image Acquisition

Participants in this study completed MRI on a 3 Tesla Siemens Prisma scanner without sedation. High resolution structural images were acquired using a 3D localizer, T1-weighted sequence, and T2-weighted transverse sequence. The T1-weighted magnetization prepared rapid gradient echo (MPRAGE) was attained with single-shot slice acquisition in the anterior-posterior direction. This consisted of 176 slices, with a TR = 1950ms, TE = 4.44ms, FOV = 256 × 256, voxels = $1mm^3$, and flip angle 12°, aligned to the AC-PC plane. The T2 sequence parameters used traverse orientation consisting of 60 slices, a TR = 4000ms, TE = 56ms, FOV = 240mm, voxels = $2mm^3$, and flip angle 170°.

Resting-state functional connectivity was quantified based on a 48-slice transverse acquisition, with anterior to posterior phase encoding, while participants rested with their eyes open and viewing a fixation cross. Sequence parameters included TR = 2000ms, TE = 28ms, FOV = 240mm, voxels $3mm^3$, and a 70° flip angle.

Volumetric Image Post-Processing

Prior to analyses, all images were examined for artifact or other unexpected irregularities. Volumetric data were post-processed using FreeSurfer 6.0 pipelines (http://surfer.nmr.mgh.harvard.edu/), including co-registration, normalization, and motion correction preprocessing protocols, for use in resting-state analyses described below.

CONN Toolbox

Resting-state fMRI was analyzed using the CONN Toolbox v18b,[17] which processes and analyzes magnetic resonance imaging data using MATLAB_R2019b and SPM12 platforms. In this study, the CONN Toolbox was first applied to analyze resting-state data (rsfMRI) using ROI-to-ROI analyses of regions prescribed based on CONN Toolbox-integrated masks of the SN, CEN, and DMN. Images first underwent preprocessing that included realignment, slice-timing correction, co-registration, normalization, and spatial and temporal smoothing with an 8mm Gaussian kernel. Since resting state data is susceptible to linear drifts and motion effects, images also underwent denoising before moving onto 1^{st} level analysis and group-level (or 2^{nd} level) analysis, and outliers were scrubbed. Additional noise components, including blood-oxygen level dependent (BOLD) signal from cerebral white matter and cerebrospinal fluid, was also removed before seed-based analyses were conducted. We then generated within- and cross-network ROI-to-ROI connectivity maps for three reproducibly demonstrated functional networks: the SN, CEN, and DMN. Seeds were 10mm diameter spheres, and the spatial coordinates and location of the seeds used in analyses are provided in Supplementary Table 3 and depicted in Figure 1a–c. These seeds

are pre-embedded in the CONN Toolbox software, and methods of identification of these seeds are provided by the developers of the toolbox.[17] Individual participants' ROI-to-ROI correlation maps were generated by extracting the average resting state BOLD time course from each seed region and calculating correlation coefficients with the average BOLD time course in the yolked ROI. These coefficients were then normalized using Fisher's r-to-z transformation. These maps were integrated across participants and used in second level analyses of group differences (voxel-wise analysis p(uncorrected) <.001 and cluster-level p(FDR corrected) < .05), and extracted and integrated into the larger SPSS database for correlation with neurocognitive assessment measures.

Statistical Analysis

One-way analysis of variance (ANOVA) was used to analyze group differences on cognitive tests and parent report measures. Because of small sample sizes, we sought to balance the risk of Type I and Type II error by considering both statistical significance and the magnitude of effect sizes. For group comparisons, effect sizes (partial eta-squared) focused on medium and large effects ($\eta^2 \geq 0.06$and $\eta^2 \geq 0.14$, respectively).[18] One-way ANOVA also examined group differences in cross-region connectivity based on the Fisher transformed connectivity correlations from the rsfMRI analyses, focusing again on medium and large effects.

To examine the relationships among neural markers and cognitive tests and parent report measures, we used pooled within-group correlations. To conserve statistical power, we focused these analyses of cross-domain associations on areas of either a) notable group difference (i.e., large effect size) *or* b) mutual connectivity (i.e., groups showing medium or larger ROI-to-ROI connectivity) on rsfMRI analysis. For each analysis, due to limited power, we again focused on medium ($r \geq .30$) and large ($r \geq .50$) correlations[18] for the purposes of interpretation, and relied on the following composite measures of cognitive function: WISC-IV Processing Speed Index, TEA-Ch subtest scaled scores, and BRIEF Behavioral Regulation Index, Metacognition Index, Global Executive Composite. Raw data are available from the corresponding author (KRH) upon request, in adherence with IRB and research institute policies on data use and release.

RESULTS

Group differences in neuropsychological measures and network connectivity

Group differences in performance on cognitive tests are presented in Table 2. The overall group comparison demonstrated at least medium effect sizes for all outcome measures, but reached statistical significance only for the WISC-IV Processing Speed Index and TEA-Ch Walk Don't Walk and Creature Counting subtests. PBTS who only underwent surgical resection performed most poorly on most neuropsychological measures. Individual patient-level performance on the TEA-Ch and WISC-IV for PBTS are also provided in Supplementary Table 2. Parent ratings on the BRIEF did not differ by group, although mean scores for both the PBTS surgery-only group and healthy control group each approached or exceeded a full standard deviation above the normative mean, reflecting elevated difficulties

in day-to-day behavioral regulation and metacognition. Mean ratings for the PTBS who also underwent adjuvant treatment were in the same direction but less pronounced.

The Fisher-transformed r-to-z correlations among network regions (Table 3) revealed no significant overall group differences in ROI-to-ROI connectivity in the SN or CEN at the specified threshold; in contrast, group differences were significant in the DMN, with PBTS in both surgery only and surgery+adjuvant treatment groups showing greater connectivity than the HC between the medial prefrontal cortex and posterior cingulate cortex. While not statistically significant in the overall ANOVA, planned contrasts identified several other significant pairwise group differences. Specifically, HC had greater connectivity in the SN between the anterior cingulate and right-hemisphere supramarginal gyrus relative to PBTS who had both surgical resection and adjuvant treatment. In contrast, PBTS had more robust connectivity in the DMN than HC, particularly connections to the medial prefrontal cortex. Several correlations showed effect sizes for all groups exceeded medium magnitude, suggesting similar connectivity between these regions (see Table 3). Group-derived ROI-to-ROI connectivity maps are depicted in Figures 2–4, with seed regions defined using the coordinates listed in Supplementary Table 3.

Correlations among neurocognitive measures and SN connectivity

Table 4 shows pooled within-group correlations among r-to-z connectivity in regions of either group differences or cross-group connectivity in the SN, DMN, and CEN and performance on neurocognitive assessment measures. In general, higher SN connectivity, particularly among the anterior cingulate cortex, anterior insula, and supramarginal gyrus, was associated with better neurocognitive task performance, but was not robustly related to parent-rated behavioral regulation and overall executive skills on the BRIEF. Within the DMN, higher connectivity between the posterior cingulate cortex and both the medial and lateral prefrontal cortex were also associated with better neurocognitive task performance, whereas higher connectivity to the medial prefrontal cortex specifically was associated with better parent-rated executive skills. In contrast, the opposite pattern was observed for connectivity in the CEN, such that greater connectivity was associated with poorer parent-rated day-to-day executive function.

DISCUSSION

PTBS often demonstrate late effects that include deficits in executive function, processing speed, memory, and attention, which can impact their academic achievement, overall adjustment, and quality of life.[3, 4, 19] This pilot study sought to examine the associations among network connectivity within the SN, CEN, and DMN and neurocognitive functioning.

As hypothesized, PTBS performed more poorly than HC on several measures of neurocognitive function, including measures of processing speed, divided attention, and executive function. Specifically, PTBS performed significantly worse on WISC-IV Processing Speed and more poorly on the Creature Counting subtest of the TEA-Ch than did HC, and a non-significant but medium effect was found for the Code Transmission subtest. An unexpected pattern emerged on the TEA-Ch Walk Don’t Walk subtest and on

parent-rated day-to-day executive skills on the BRIEF, with PBTS who only underwent surgical resection performing particularly poorly. While adjuvant treatment is often linked with poorer outcome following pediatric brain tumor, in this small sample, performance deficits were more remarkable and parent rated executive function further from normative expectation relative to healthy peers or those who underwent both surgery and additional treatment. This highlights a need for close attention to long term sequelae, even in those spared the neurotoxicity of intrathecal chemotherapy and cranial radiation. While neurotoxic risk is often discussed in conjunction with adjuvant treatment approaches, particularly cranial radiation,[21,22] others have shown that treatment with surgery only conveys some risk of neurocognitive and behavioral late effects.[23,24]

While no significant group differences were found in parent-rated day-to-day executive skills on the BRIEF, scores for both the PBTS surgery-only and HC groups generally were at least a full standard deviation above the normative mean, suggesting the lack of group differences may be driven by unexpectedly poor ratings for HC. Overall, these findings are consistent with past research on cognitive deficits in PTBS,[4] but suggest potential bias in children from the HC group who elected to complete MRI in addition to the larger parent study. In fact, exploratory analyses found that HC who participated in the MRI study were rated by parents as having poorer behavioral regulation and overall executive skills on the BRIEF (ps < .05), though performance on the TEA-Ch and WISC Processing Speed did not differ based on MRI study participation.

Group differences in within-network connectivity followed a generally consistent pattern: PBTS demonstrated greater connectivity across ROIs in the DMN, particularly the anterior portion of the DMN. This pattern is consistent with prior research that found evidence of an inability to efficiently disengage the DMN following other forms of acquired brain injury (e.g., TBI).[25] This inability to disengage may result in inefficient cognitive control and has been linked with poorer performance on neurocognitive measures. In this sample, however, PBTS were prone to heightened connectivity in the DMN, which was then associated with better performance-based and parent-rated executive function. This is more consistent with the findings of Chen and colleagues, who found more expansive connectivity in adult brain tumor survivors.[13] Notably, they used an independent component analysis approach, whereas we used a functional network atlas approach because of our small sample. Given this difference, the extent to which our findings replicate the compensatory engagement of regions outside the typical network atlas found by Chen et al. is uncertain.

The reasons for our mixed findings are difficult to discern in a small pilot study; importantly, the sample of PBTS was heterogeneous and included many survivors of posterior fossa tumors. Therefore, the likelihood of direct damage to network connectivity, particularly in anterior regions, was lesser than would be the case with supratentorial tumors. Furthermore, the number of children in each treatment group was small. While we considered analyzing all survivors in a single group, the heterogeneity in tumor histology, location, and treatment modality are important potential moderators of outcomes. We believe grouping by treatment best reflected diagnostic risk, but we acknowledge we could have approached subgrouping in other ways.

This study has several limitations. Firstly, the small sample size (n = 23) limited our power to detect statistical significance, particularly for analyses subdivided by group. We opted against correcting for multiple comparisons to avoid being overly conservative and risking Type II error in an exploratory context, but acknowledge that these findings are preliminary and require replication. The small sample size also made it difficult to examine whether group differences in performance were, for example, mediated by any of the neural markers we examined. This is a planned area for further examination in a larger sample. Secondly, study participants were limited to those who could remain still during MRI; because children who are unable to remain still for the MRI may include more significantly impaired survivors, particularly among those who received adjuvant treatment, this may have reduced variability in both MRI metrics and neurocognitive functioning. That said, overall performance on the neurocognitive measures mirrored meta-analytic findings regarding cognitive impairment following pediatric brain tumor.[4] The sample also was drawn from only one location, and included White children and parents almost exclusively. Thus, our findings may not generalize to the broader population of PBTS or more diverse samples, and highlight the importance of multi-institutional collaboration and team science. Unknown sample biases in the HC group could have impacted both neurocognitive functioning and MRI completion; indeed, we found that the HC performed more poorly than expected on one of the TEA-Ch subtests and were rated more poorly by parents in day-to-day executive skills, based on normative comparisons. Parents of HC who had concerns about cognitive function may have been more likely to agree to participate in a MRI study, and therefore may not be fully representative of the broader population of healthy children and adolescents. Of course, this would bias against finding group differences, yet the HC performed more poorly than the PTBS in several cognitive domains.

Despite these limitations, this study adds to the scant literature on functional connectivity and its relationships with neurocognitive outcomes following pediatric brain tumor. We intend to expand this work in several ways in the future: in a larger, multi-site study, allowing for examination of mechanisms underlying these correlations; and in a longitudinal approach beginning closer to diagnosis and treatment, allowing for study of the temporal cascade of both brain system changes and evolution of neurocognitive function.

Supplementary Material

Refer to Web version on PubMed Central for supplementary material.

ACKNOWLEDGEMENTS

This work was supported by a Supportive Care Grant from the St. Baldrick's Foundation to Kristen R. Hoskinson, PhD, and from the National Cancer Institute (R01 CA172723-01) to Kathryn Vannatta, PhD. We appreciate the contributions of research staff who facilitated data collection, including Ryan Wier, Holly Aleksonis, Sandra Glazer, Hanan Guzman, Mary Hagan, Payton Hagerdorn, Emily Meadows, Eric Semmel, and Katie Ballistreri. These efforts would not have been possible without the generous time and effort of the families who participated.

REFERENCES

1. Johnson KJ, Cullen J, Barnholtz-Sloan JS, et al. Childhood Brain Tumor Epidemiology: A Brain Tumor Epidemiology Consortium Review. Cancer Epidemiology, Biomarkers, & Prevention. 2014;23(12):2716–2736.
2. Ostrom QT, Cioffi G, Gittleman H, et al. CBTRUS Statistical Report: Primary Brain and Other Central Nervous System Tumors Diagnosed in the United States in 2012–2016. Neuro-oncology. 2019;21(Suppl 5):v1–v100. [PubMed: 31675094]
3. Ris MD, Noll RB. Long-term neurobehavioral outcome in pediatric brain-tumor patients: review and methodological critique. J Clin Exp Neuropsychol. 1994;16(1):21–42. [PubMed: 8150888]
4. Robinson KE, Kuttesch JF, Champion JE, et al. A Quantitative Meta-Analysis of Neurocognitive Sequelae in Survivors of Pediatric Brain Tumors. Pediatric Blood & Cancer. 2010;55(3):525–531. [PubMed: 20658625]
5. Craig AD. How do you feel--now? The anterior insula and human awareness. Nat Rev Neurosci. 2009;10(1):59–70. [PubMed: 19096369]
6. Gogolla N, Takesian AE, Feng G, et al. Sensory integration in mouse insular cortex reflects GABA circuit maturation. Neuron. 2014;83(4):894–905. [PubMed: 25088363]
7. Menon V, Uddin LQ. Saliency, switching, attention and control: a network model of insula function. Brain Struct Funct. 2010;214(5–6):655–667. [PubMed: 20512370]
8. Menon V Salience Network. In Toga AW, (Ed). Brain Mapping: An Encyclopedic Reference: Press: Elsevier 2015:597–611.
9. Sridharan D, Levitin DJ, Menon V. A critical role for the right fronto-insular cortex in switching between central-executive and default-mode networks. Proc Natl Acad Sci U S A. 2008;105(34):12569–12574. [PubMed: 18723676]
10. Bressler SL, Menon V. Large-scale brain networks in cognition: emerging methods and principles. Trends Cogn Sci. 2010;14(6):277–290. [PubMed: 20493761]
11. Lv H, Wang Z, Tong E, Williams LM, Zaharchuk G, Zeineh M, Goldstein-Piekarski AN, Ball TM, Liao C, Wintermark M. Resting-state functional MRI: Everything that nonexperts have always wanted to know. American Journal of Neuroradiology. 2018;39(8):1390–1399. [PubMed: 29348136]
12. Anandarajah H, Seitzman BA, McMichael A, et al. Cognitive Deficits and Altered Functional Brain Network Organization in Pediatric Brain Tumor Patients. 2020.
13. Chen HB, Wang LY, King TZ, et al. Increased frontal functional networks in adult survivors of childhood brain tumors. Neuroimage-Clinical. 2016;11:339–346. [PubMed: 27298763]
14. Wechsler D WISC-IV: Wechsler Intelligence Scale for Children (4th Ed.). San Antonio, TX: The Psychological Corporation 2003.
15. Evans AS, Preston AS. Test of Everyday Attention for Children. In Kreutzer JS, DeLuca J, Caplan B, (Eds). Encyclopedia of Clinical Neuropsychology. New York, NY: Springer 2011.
16. Gioia GA, Isquith PK, Guy SC, et al. TEST REVIEW Behavior Rating Inventory of Executive Function. Child Neuropsychology. 2010;6:235–238.
17. Whitfield-Gabrieli S, Nieto-Castanon A. Conn: a functional connectivity toolbox for correlated and anticorrelated brain networks. Brain Connect. 2012;2(3):125–141. [PubMed: 22642651]
18. Cohen J Statistical Power Analysis for the Behavioral Sciences. New York, NY: Routledge Academic 1988.
19. Wolfe KR, Madan-Swain A, Kana RK. Executive Dysfunction in Pediatric Posterior Fossa Tumor Survivors: A Systematic Literature Review of Neurocognitive Deficits and Interventions. Developmental Neuropsychology. 2012;37(2):153–175. [PubMed: 22339228]
20. Aleksonis HA, Wier R, Pearson MM, et al. Associations among diffusion tensor imaging and neurocognitive function in survivors of pediatric brain tumor: A pilot study. Applied Neuropsychology-Child.
21. Kahalley LS, Ris MD, Mahajan A, et al. Prospective, longitudinal comparison of neurocognitive change in pediatric brain tumor patients treated with proton radiotherapy versus surgery only. Neuro-Oncology. 2019;21(6):809–818. [PubMed: 30753584]

22. Ramirez-Guerrero S, Vargas-Cuellar MP, Charry-Sanchez JD, Talero-Gutierrez C. Cognitive sequelae of radiotherapy in primary brain tumors. Interdisciplinary Neurosurgery. 2021;26:1–9.

23. Ris MD, Beebe DW, Armstrong FD, et al. Cognitive and adaptive outcome in extracerebellar low-grade brain tumors in children: A report from the Children's Oncology Group. Journal of Clinical Oncology. 2008;26:4765–4770. [PubMed: 18779602]

24. DiRocco C, Chieffo D, Pettoroni BL, et al. Preoperative and postoperative neurological, neuropsychological, and behavioral impairment in children with posterior cranial fossa astrocytomas and medulloblastomas: The role of the tumor and the impact of the surgical treatment. Childs Nervous System. 2010;26:1173–1188.

25. Bonnelle V, Ham TE, Leech R, et al. Salience network integrity predicts default mode network function after traumatic brain injury. Proc Natl Acad Sci U S A. 2012;109(12):4690–4695. [PubMed: 22393019]

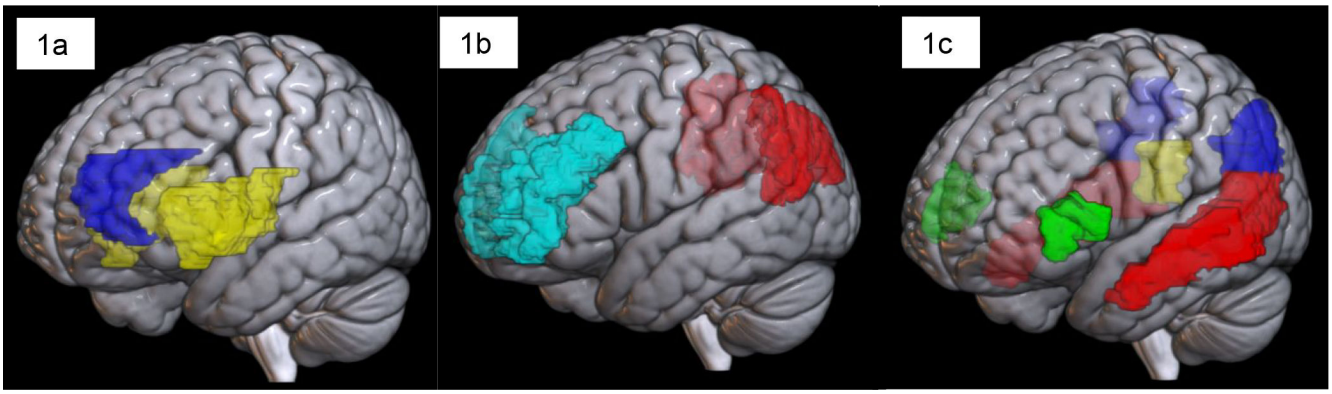

Figure 1.

Functional Network Core Locations

Note: In Figure 1a (Salience Network), yellow indicates anterior insula and blue indicates anterior cingulate cortex. In Figure 1b (Central Executive Network), cyan indicates dorsolateral prefrontal cortex and red indicates posterior parietal cortex. In Figure 1c (Default Mode Network), blue indicates angular gyrus, red indicates medial temporal lobe, green indicates ventromedial prefrontal cortex, and yellow indicates posterior cingulate cortex.

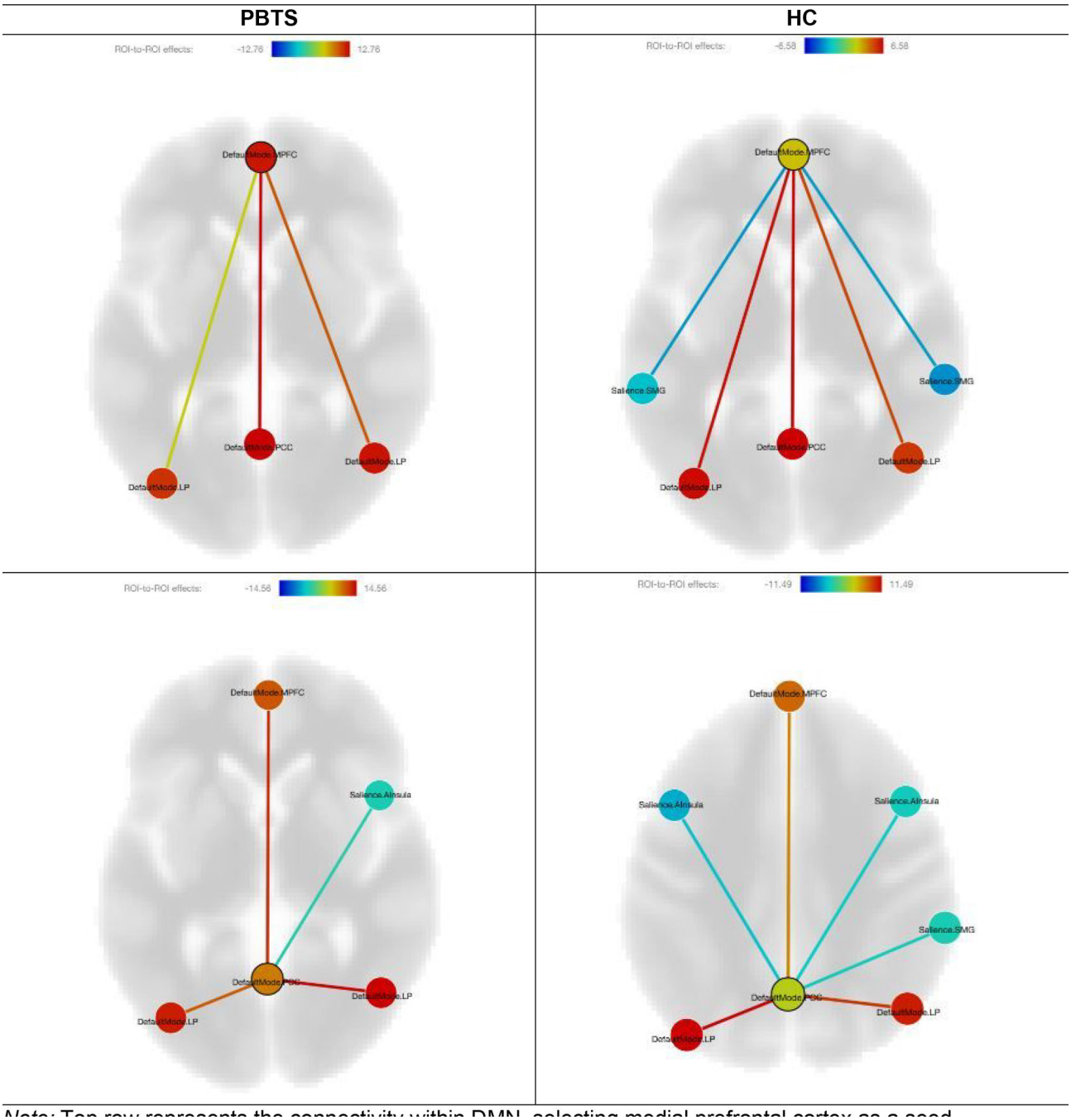

Note: Top row represents the connectivity within DMN, selecting medial prefrontal cortex as a seed.

Figure 2.

ROI-to-ROI Connectivity in Default Mode Network Among PBTS and HC

Note: Top row represents the connectivity within DMN, selecting medial prefrontal cortex as a seed.

Bottom row represents the connectivity within DMN, selecting posterior cingulate cortex as a seed.

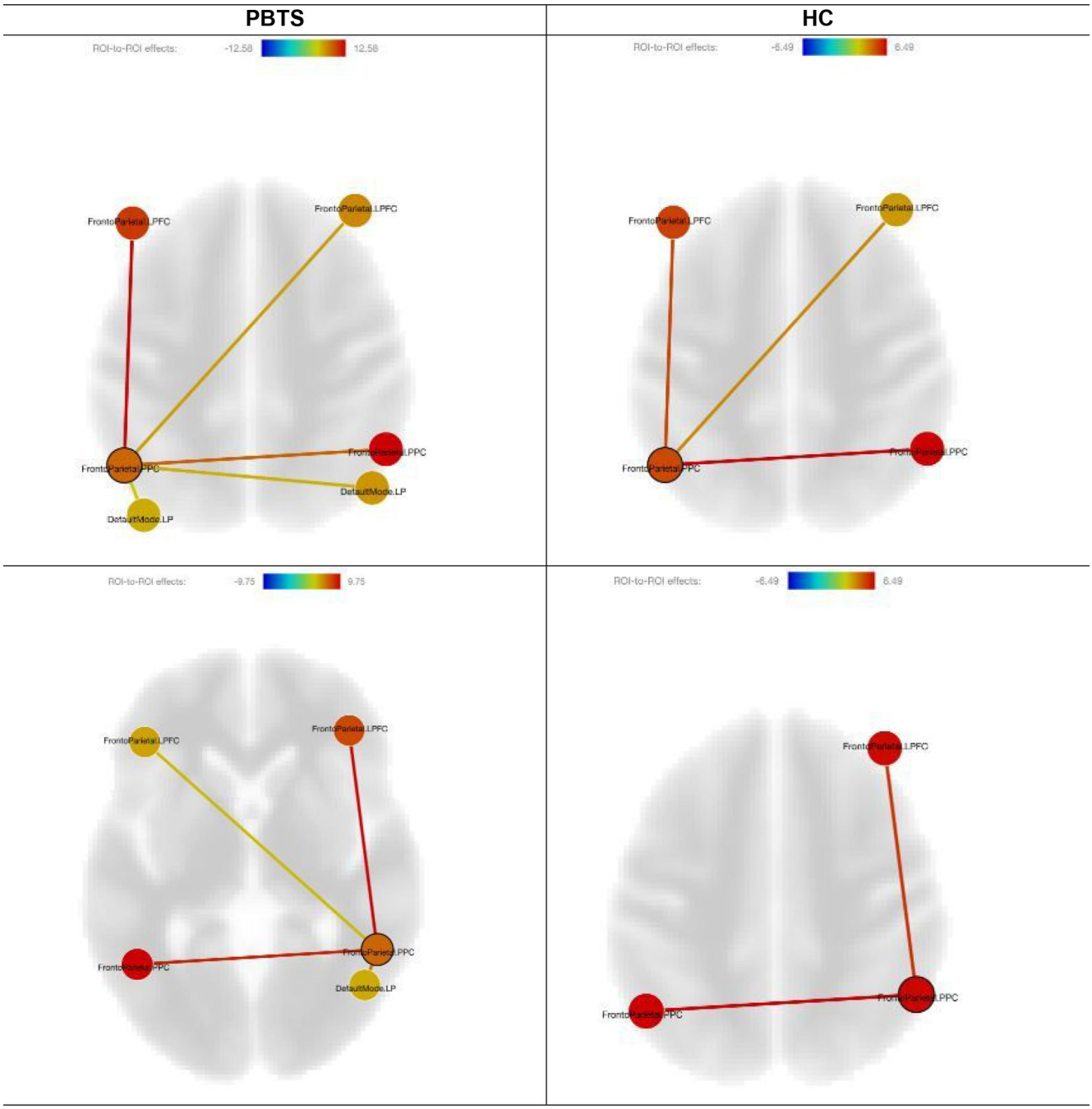

Figure 3.

ROI-ROI Connectivity in Central Executive Network Among PBTS and HC

Note: Top row represents the connectivity within CEN, selecting left posterior parietal cortex as a seed.

Bottom row represents the connectivity within CEN, selecting right posterior parietal cortex as a seed.

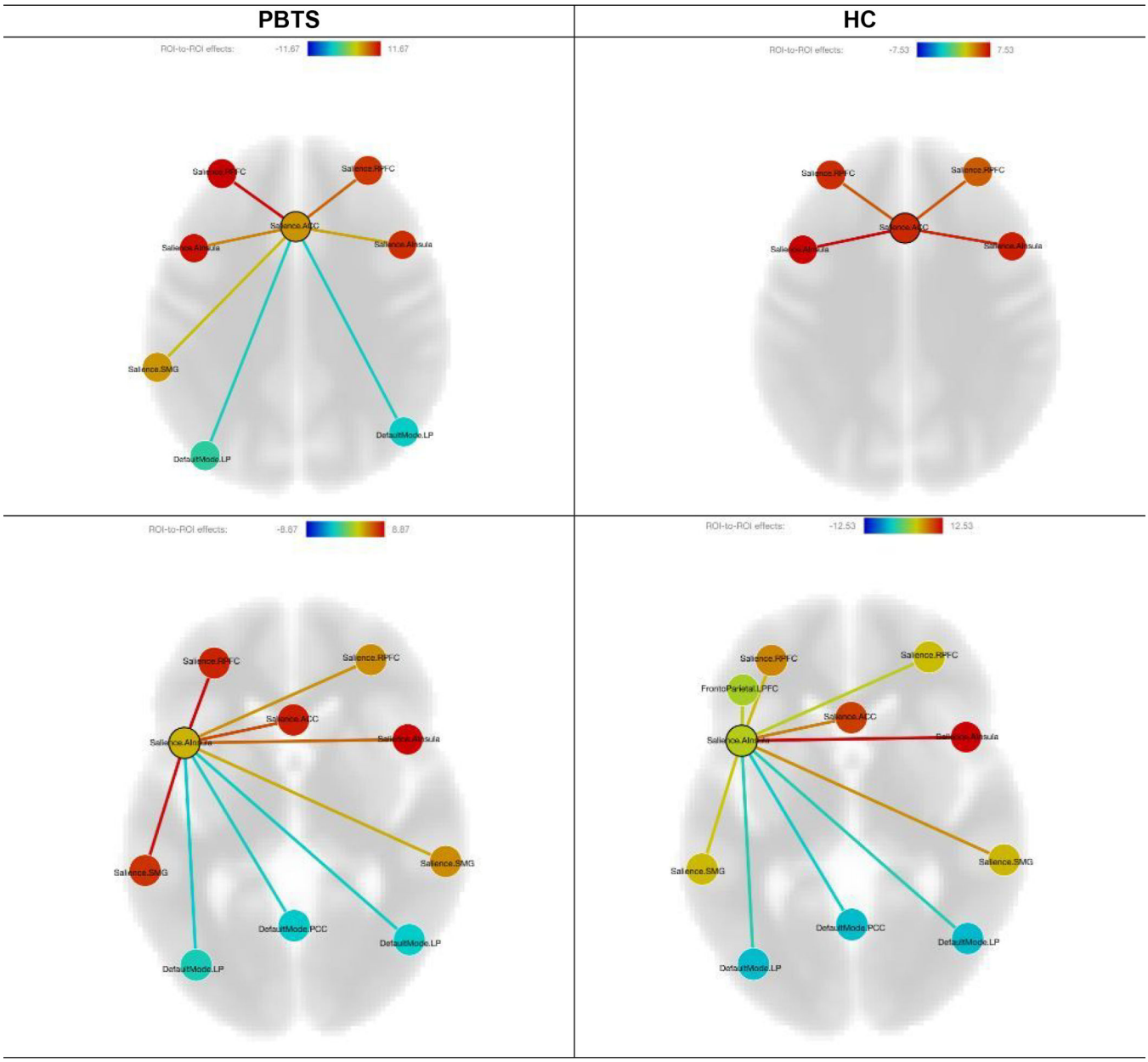

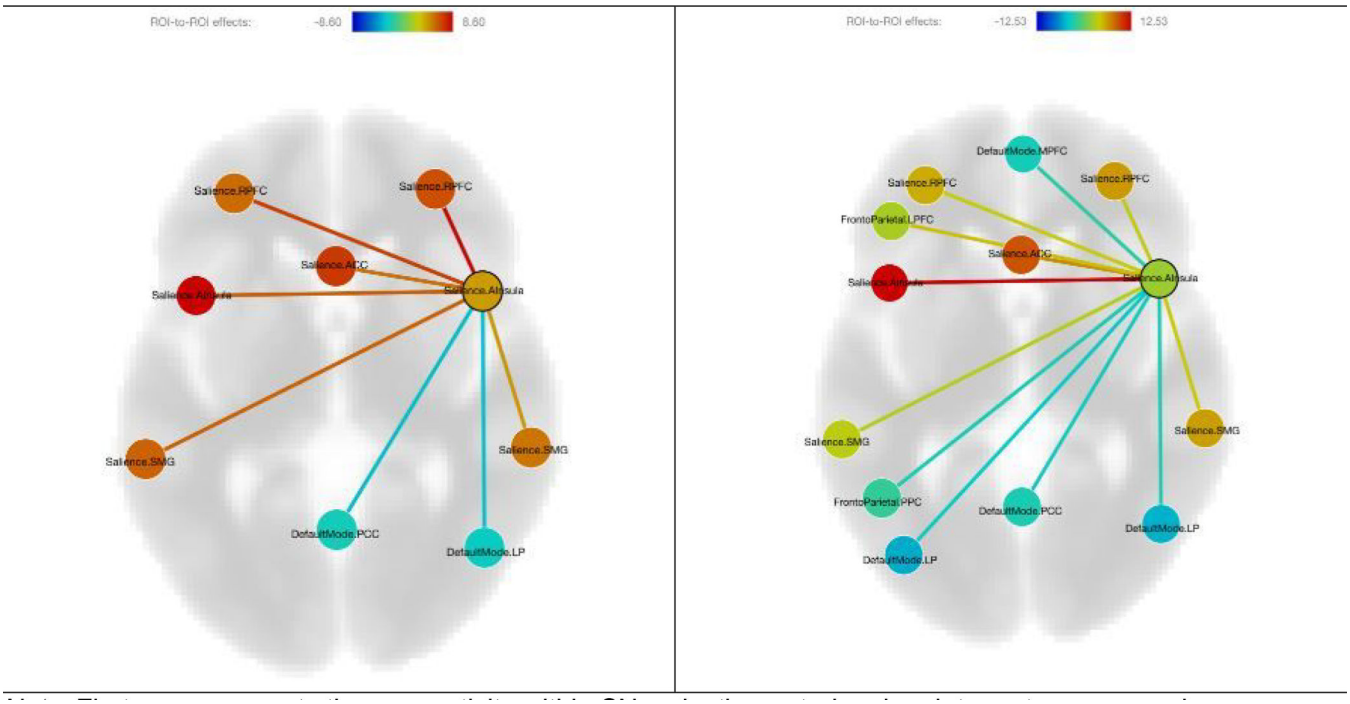

Figure 4.

ROI-ROI Connectivity in Salience Network Among PBTS and HC

Note: First row represents the connectivity within SN, selecting anterior cingulate cortex as a seed.

Second row represents the connectivity within SN, selecting left anterior insula as a seed.

Third row represents the connectivity within SN, selecting right anterior insula as a seed.

Table 1.

Group Demographic Comparison and Diagnostic/Treatment Characteristics

	PBTS-Sg (*n* = 7) *M (SD)*	PBTS-Sg+A (*n* = 6) *M (SD)*	HC (*n* = 10) *M (SD)*	*F/t/X*^{2}	*p*
Demographic Characteristics					
Age at testing (years)	12.24 (2.74)	13.36 (2.56	12.70 (2.20)	0.33	.720
Male (*n*, %)	4 (57.1%)	5 (83.3%)	6 (60.0%)	1.19	.552
White (*n*, %)	6 (85.7%)	6 (100.0%)	10 (100.0%)	2.39	.303
Non-Hispanic (*n*, %)	7 (100.0%)	6 (100.0%)	9 (90.0%)	1.36	.507
Family income > $75,000 (*n*, %)	4 (57.1%)	3 (50.0%)	8 (80.0%)	2.12	.346
Marital status: Partnered (*n*, %)	6 (85.7%)	5 (83.3%)	9 (90.0%)	0.16	.923
Parent years of education	15.71 (1.70)	14.67 (1.97)	15.90 (2.92)	0.54	.594
Diagnostic/Treatment Characteristics					
Time since diagnosis (years)	7.08 (2.14)	7.91 (4.16)	-	−0.47	.650
Time off treatment (years)	6.05 (1.73)	5.98 (2.72)	-	0.09	.929
Tumor histology					
Astrocytoma	4 (57.1%)	0 (0.0%)	-	8.98	.030
Medulloblastoma	0 (0.0%)	4 (66.7%)	-		
Ganglioglioma	2 (28.6%)	2 (33.3%)	-		
Glioneuronal	1 (14.3%)	0 (0.0%)	-		
Tumor location					
Infratentorial	2 (28.6%)	4 (66.7%)	-	2.27	.321
Supratentorial	4 (57.1%)	2 (33.3%)	-		
Midbrain Tectal	1 (14.3%)	0 (0.0%)	-		
Treatment modality					
Surgical resection (*n*, %)	7 (100.0%)	6 (100.0%)	-		
Chemotherapy	0 (0.0%)	4 (66.7%)	-		
Cranial Radiation	0 (0.0%)	5 (83.3%)	-		

Note: PBTS = pediatric brain tumor survivors; Sg = surgery only; Sg+A = surgery plus adjuvant treatment; HC = healthy children; *M* = mean; *SD* = standard deviation.

Table 2.

Group Differences in Neuropsychological Assessment Performance

	PBTS-Sg *M (SD)*	PBTS-Sg+A *M (SD)*	HC *M (SD)*	*F*	*p*	Eta^2
WISC-IV						
Coding scaled score	6.86 (2.91)	6.83 (2.14)	9.60 (2.76)	3.02[a]	.072	.23
Symbol Search scaled score	9.71 (1.80)	10.17 (2.48)	11.90 (2.28)	2.34	.122	.19
PSI Composite score	90.29 (13.18)	91.33 (12.55)	104.50 (11.34)	3.58[ab]	.047	.26
TEA-Ch						
Walk Don't Walk[†]	3.71 (2.29)	9.67 (5.43)	7.90 (3.11)	7.27[ac]	.026	.33
Code Transmission	8.57 (2.51)	9.67 (4.84)	10.90 (2.02)	1.18	.328	.11
Creature Counting	6.43 (1.90)	7.33 (2.58)	10.20 (2.49)	5.99[ab]	.009	.37
BRIEF						
Behavioral Regulation	64.86 (13.03)	52.83 (11.84)	58.10 (8.20)	2.05	.156	.17
Metacognition	66.57 (13.77)	57.67 (13.31)	60.20 (8.77)	1.05	.368	.10
Global Executive	67.00 (14.40)	56.67 (13.57)	60.10 (8.28)	1.33	.286	.12

Note: PBTS = pediatric brain tumor survivors; Sg = surgery only; Sg+A = surgery plus adjuvant treatment; HC = healthy children; *M* = mean; *SD* = standard deviation; WISC-IV = Wechsler Intelligence Scale for Children-Fourth Edition; PSI = Processing Speed Index; TEA-Ch = Test of Everyday Attention for Children; BRIEF = Behavior Rating Inventory of Executive Function.

[†]Distribution for the Walk Don't Walk subtest failed the assumption of homogeneity of variance, so group comparison used the Kruskal-Wallis nonparametric approach and effect size was calculated using epsilon squared.

[a]PBTS-Sg≠HC

[b]PBTS-Sg+A≠HC

[c]PBTS-Sg≠PBTS-Sg+A

Table 3.

Group Differences in ROI to ROI Within-Network Connectivity (Fisher z)

	PBTS-Sg *M (SD)*	PBTS-Sg+A *M (SD)*	HC *M (SD)*	*F*	*p*	Eta^2
Salience Network						
ACC_AI-L	0.448 (.197)	0.722 (.208)	0.717 (.390)	1.59	.237	.18$^{\wedge}$
ACC_AI-R	0.445 (.164)	0.700 (.425)	0.541 (.426)	0.60	.560	.07
ACC_RPFC-L	0.568 (.271)	0.630 (.219)	0.647 (.297)	0.15	.864	.02^{+}
ACC_RPFC-R	0.441 (.196)	0.480 (.175)	0.617 (.299)	0.98	.398	.12
ACC_SMG-L	0.099 (.217)	0.253 (.219)	0.217 (.257)	0.64	.543	.08
ACC_SMG-R	−0.006 (.254)	0.285 (.292)	0.316 (.181)	3.62^{a}	.052	.33$^{\wedge}$
AI-L_AI-R	0.611 (.301)	0.696 (.379)	0.866 (.288)	1.20	.329	.14$^{\wedge+}$
AI-L_RPFC-L	0.404 (.193)	0.543 (.333)	0.571 (.282)	0.71	.508	.09
AI-L_RPFC-R	0.280 (.262)	0.214 (.250)	0.414 (.221)	1.07	.368	.13
AI-L_SMG-L	0.500 (.168)	0.337 (.116)	0.423 (.270)	1.77	.413	.10
AI-L_SMG-R	0.284 (.200)	0.233 (.314)	0.464 (.159)	2.05	.163	.22$^{\wedge}$
AI-R_RPFC-L	0.341 (.166)	0.357 (.308)	0.407 (.299)	0.12	.891	.02
AI-R_RPFC-R	0.451 (.197)	0.311 (.253)	0.477 (.303)	0.56	.581	.07
AI-R_SMG-L	0.360 (.243)	0.247 (.218)	0.249 (.291)	0.37	.699	.05
AI-R_SMG-R	0.239 (.268)	0.505 (.284)	0.465 (.332)	1.27	.309	.15$^{\wedge}$
Default Mode Network						
MPFC_LP-L	0.362 (.262)	0.703 (.288)	0.359 (.262)	2.99^{bc}	.081	.29$^{\wedge}$
MPFC_LP-R	0.468 (.092)	0.551 (.272)	0.290 (.171)	3.42^{b}	.060	.31$^{\wedge}$
MPFC_PCC	0.588 (.175)	0.593 (.140)	0.274 (.296)	4.02^{ab}	.040	.35$^{*\wedge}$
PCC_LP-L	0.752 (.251)	0.661 (.159)	0.656 (.377)	0.19	.829	.03^{+}
PCC_LP-R	0.753 (.119)	0.652 (.142)	0.631 (.308)	0.50	.615	.06^{+}
Central Executive Network						
PPC-L_LPFC-L	0.567 (.267)	0.690 (.206)	0.583 (.261)	0.32	.731	.04^{+}
PPC-L_LPFC-R	0.373 (.278)	0.520 (.120)	0.282 (.251)	1.31	.299	.15$^{\wedge}$
PPC-L_PPC-R	0.698 (.210)	0.696 (.092)	0.765 (.338)	0.15	.864	.02^{+}
PPC-R_LPFC-L	0.322 (.338)	0.327 (.087)	0.362 (.270)	0.04	.958	.01
PPC-R_LPFC-R	0.530 (.216)	0.782 (.145)	0.567 (.352)	1.10	.358	.13^{+}

Note: PBTS = pediatric brain tumor survivors; Sg = surgery only; Sg+A = surgery plus adjuvant treatment; HC = healthy children; *M* = mean; *SD* = standard deviation; ACC = Anterior Cingulate Cortex; AI-L = Anterior Insula, Left Hemisphere; AI-R = Anterior Insula, Right Hemisphere; RPFC-L = Rostral Prefrontal Cortex – Left Hemisphere; RPFC-R = Rostral Prefrontal Cortex, Right Hemisphere; SMG-L = Supramarginal Gyrus, Left Hemisphere; SMG-R = Supramarginal Gyrus, Right Hemisphere; MPFC = Medial Prefrontal Cortex; LP-L = Lateral Parietal Lobe, Left Hemisphere; LP-R = Lateral Parietal Lobe, Right Hemisphere; PCC = Posterior Cingulate Cortex; PPC-L = Posterior Parietal Cortex, Left

Hemisphere; LPFC-L = Lateral Prefrontal Cortex, Left Hemisphere; LPFC-R = Lateral Prefrontal Cortex, Right Hemisphere; PPC-R = Posterior Parietal Cortex, Right Hemisphere

[*] $p < .05$

[^] large group difference effect size (i.e., Partial eta squared ≥ .14)[21]

[+] mutual/cross-group medium- or larger ROI-to-ROI connectivity (i.e., $z \geq 0.50$ *or* $z \leq -0.50$)

[†] Distribution for the Salience Network AI-L_SMG-L contrast failed the assumption of homogeneity of variance, so group comparison used the Kruskal-Wallis nonparametric approach and effect size was calculated using epsilon squared.

[a] PBTS-Sg≠HC

[b] PBTS-Sg+A≠HC

[c] PBTS-Sg≠PBTS-Sg+A

Table 4.

Pooled Within-Group Correlation of Neurocognitive Assessment and SN, DMN, and CEN Connectivity

Group Differences in r-to-z Correlation, based on statistical significance **(see Table 3)**							
	WISC-V PSI	**TEA-Ch CC**	**TEA-Ch WDW**	**TEA-Ch CT**	**BRIEF BRI**	**BRIEF MI**	**BRIEF GEC**
DMN MPFC_PCC	**.398**$^{\wedge}$	−.196	.227	−.179	**−.357**$^{\wedge}$	**−.603***	**−.526***
Group Differences in r-to-z Correlation, based on large effect of $\eta^2 \geq 0.14$ (see Table 3)							
SN ACC_AI-L	−.166	**.568***	.213	.192	−.050	−.211	−.136
SN ACC_SMG-R	**.440***	.148	**.412**$^{\wedge}$	**.413**$^{\wedge}$	−.248	−.242	−.232
SN AI-L_AI-R	.034	**−.346**$^{\wedge}$	.055	.269	−.038	−.032	−.018
SN AI-L_SMG-R	.121	.044	**.346**$^{\wedge}$	.266	.204	.195	.221
SN AI-R_SMG-R	.146	−.183	.021	.065	−.093	−.163	−.113
DMN MPFC_LP-L	.269	−.235	.028	−.295	−.226	−.280	−.254
DMN MPFC_LP-R	**.302**$^{\wedge}$	−.199	−.297	**.354**$^{\wedge}$	−.037	.054	.046
CEN PPC-L_LPFC-R	.039	.169	.085	−.023	**.524***	**.318**$^{\wedge}$	**.416***
Mutual/Cross-group Medium or Larger Effect Size in r-to-z Correlation (see Table 3)							
SN ACC_RPFC-L	**.334**$^{\wedge}$	−.222	−.192	−.003	.212	.136	.172
DMN PCC_LP-L	**.456***	−.093	**.516***	**.375**$^{\wedge}$	.010	−.248	−.138
DMN PCC_LP-R	.172	.076	.251	−.007	.250	.014	.128
CEN PPC-L_LPFC-L	−.136	**.408**$^{\wedge}$	−.198	−.078	**.434***	**.460***	**.458***
CEN PPC-L_PPC-R	.044	−.022	**.384**$^{\wedge}$	−.118	.142	.031	.072
CEN PPC-R_LPFC-R	**−.310**$^{\wedge}$	**−.248**	−.179	.023	**.335**$^{\wedge}$	.211	.284

Note: SN = Salience Network; DMN = Default Mode Network; CEN = Central Executive Network; ACC = Anterior Cingulate Cortex; AI-L = Anterior Insula, Left Hemisphere; AI-R = Anterior Insula, Right Hemisphere; RPFC-L = Rostral Prefrontal Cortex – Left Hemisphere; RPFC-R = Rostral Prefrontal Cortex, Right Hemisphere; SMG-L = Supramarginal Gyrus, Left Hemisphere; SMG-R = Supramarginal Gyrus, Right Hemisphere; MPFC = Medial Prefrontal Cortex; LP-L = Lateral Parietal Lobe, Left Hemisphere; LP-R = Lateral Parietal Lobe, Right Hemisphere; PCC = Posterior Cingulate Cortex; PPC-L = Posterior Parietal Cortex, Left Hemisphere; LPFC-L = Lateral Prefrontal Cortex, Left Hemisphere; LPFC-R = Lateral Prefrontal Cortex, Right Hemisphere; PPC-R = Posterior Parietal Cortex, Right Hemisphere

* $p < .05$

$^{\wedge}$ non-significant but medium effect size.[21]